RAPID COMMUNICATIONS

PHYSICAL REVIEW B VOLUME 44, NUMBER 2 1 JULY 1991-II

Decay processes of nonequilibrium phonons in Pr^{3+}-doped yttrium aluminum garnet

Xiao-jun Wang, Joseph Ganem, W. M. Dennis, and W. M. Yen
Department of Physics and Astronomy, University of Georgia, Athens, Georgia 30602
(Received 8 April 1991)

We have investigated the decay of nonequilibrium phonons in YAG:Pr^{3+} (1.0 at.%) at a temperature of 16 K. Nonequilibrium phonon populations are generated monochromatically with a high-power pulsed far-infrared laser using defect-induced one-phonon absorption, and their temporal and spectral evolution determined using a time-resolved vibronic sideband spectrometer. We find that two decay mechanisms dominate the nonequilibrium phonon relaxation: anharmonic decay via three-phonon interactions and two-phonon–one-electron inelastic-scattering processes. The latter mechanism leads to the evolution of a highly peaked phonon distribution that persists for several phonon generations.

The relaxation of monochromatic high-frequency phonons to a thermal distribution is generally explained in terms of anharmonic processes.[1,2] In investigating the spectral and temporal dynamics associated with the decay of narrow-band nonequilibrium phonons in YAG:Pr^{3+} (where YAG is yttrium aluminum garnet), we observe that for phonons of wave number less than 60 cm^{-1}, the dominant relaxation mechanism is inelastic scattering by electronic states (23 and 43 cm^{-1}) of Pr^{3+} ions located in distorted sites. Inelastic phonon scattering leads to the evolution of a highly peaked phonon distribution which persists for times much greater than the lifetime of the initial narrow-band phonons.

In this work, we use defect-induced one-phonon absorption (DIOPA) of far-infrared (FIR) radiation to generate monochromatic phonons[3] at a range of wave numbers between 30 and 113 cm^{-1} in YAG:Pr^{3+} with a frequency bandwidth limited by the FIR laser of < 500 MHz. Phonon detection with both spectral and temporal resolution is achieved using a variation on the anti-Stokes absorption sideband spectrometer. Phonons of arbitrary energy Δ can be detected by measuring the absorption of a tunable dye laser, which is detuned by Δ from the Pr^{3+} $^3H_4$-$^3P_0$ transition. In practice, this absorption is monitored by measuring the $^3P_0$-$^3H_6$ time-integrated fluorescence. The temporal evolution of the phonon population is obtained by delaying the tunable phonon detection laser pulse with respect to the FIR phonon generation pulse.

Figure 1(a) shows the relevant energy levels for generation and resonant detection of nonequilibrium phonons in YAG:Pr^{3+}. The dashed line represents the phonon population generated by DIOPA at energy Δ.

The nonequilibrium phonon occupation number is usually calculated from the ratio of the anti-Stokes absorption in the presence of a nonequilibrium phonon population to the Stokes absorption in the absence of nonequilibrium phonons at low temperature ($\Delta \gg kT$).[4] At our sample temperature of 16 K, the condition $\Delta \gg kT$ is no longer satisfied. However, at this temperature an anti-Stokes calibration can be obtained when the dye laser pulse is incident on the sample before the FIR pulse. We therefore normalize to the anti-Stokes absorption sideband in the following manner. The phonon induced absorption in the presence of a nonequilibrium phonon population is given by

$$\alpha(\Delta) = C[n_{\rm non}(\Delta) + n_{\rm th}(\Delta)] \sum_{\lambda} \rho(\Delta,\lambda) F(\Delta,\lambda) , \qquad (1)$$

where $n_{\rm non}(\Delta)$ and $n_{\rm th}(\Delta)$ are nonequilibrium and thermal occupation numbers at phonon energy Δ, respectively; $\rho(\Delta,\lambda)$ is the phonon density of states at frequency Δ and polarization branch λ, $F(\Delta,\lambda)$ is the electron-phonon coupling strength, and C is a constant. The nonequilibrium

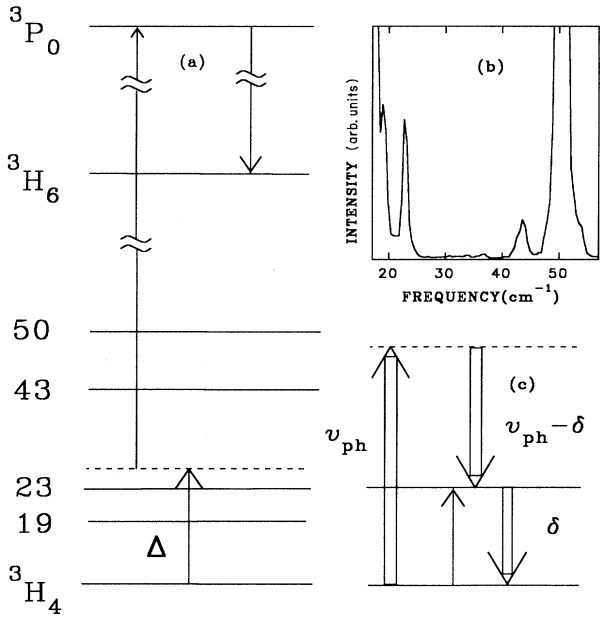

FIG. 1. (a) Energy-level diagram of YAG:Pr^{3+} showing the states utilized for the anti-Stokes absorption sideband spectrometer. Δ is the detuning of the dye laser from the $^3H_4$-$^3P_0$ zero-phonon transition. The position of low-lying crystal-field split states are shown for Pr^{3+} ions in both undistorted (19 and 50 cm^{-1}) and distorted (23 and 43 cm^{-1}) sites. (b) Anti-Stokes excitation spectrum of $^3P_0$ at 16 K obtained by monitoring the $^3P_0$-$^3H_6$ fluorescence. (c) Schematic representation of inelastic scattering: a phonon of frequency ν_{ph} causes an electronic transition with frequency δ generating a phonon at the difference frequency (ν_{ph}-δ). The electronic excitation further relaxes by emission of a phonon of frequency δ.

phonon occupation number is then calculated using

$$n_{\text{non}}(\Delta) = n_{\text{th}}(\Delta, T)\frac{\alpha(\Delta) - \alpha_{\text{th}}(\Delta)}{\alpha_{\text{th}}(\Delta)}, \quad (2)$$

where

$$\alpha_{\text{th}}(\Delta) = Cn_{\text{th}}(\Delta)\sum_{\lambda}\rho(\Delta,\lambda)F(\Delta\lambda)$$

is the absorption due to the thermal phonons and $n_{\text{th}}(\Delta)$ is the Planck distribution at the sample temperature T.

The details of the experimental setup required to implement these techniques have been described in Refs. 5 and 6. Our experiment differs from that of the above references in that the $3\times3\times6$ mm^3 YAG:Pr^{3+} (1 at.%) single crystal is mounted on the cold finger of a two stage closed-cycle refrigerator. The sample temperature was determined to be 16 K, by comparing the line strengths of transitions from the two lowest levels of the ground-state manifold to the $^3P_0$.

In interpreting the phonon spectra it is necessary to consider the details of the excitation spectrum shown in Fig. 1(b). In addition to the previously reported crystal-field-split lines at 19 and 50 cm^{-1}, we observe two additional peaks at 23 and 43 cm^{-1}. The absence of similar peaks on the Stokes side of the zero-phonon transition suggests that they are not due to low-lying optical phonons. Pumping of the $^3P_0$ from these states at 16 K produced fluorescence spectra which are similar to that of the undistorted Pr^{3+} in general, but differ in the positions of the crystal-field sublevels. We therefore believe these peaks to be due to either electronic levels in the ground-state manifold of Pr^{3+} ions which are located in distorted sites or alternatively Pr^{3+} pair states.

Figure 2 shows the phonon spectra at a range of times after phonon generation at 113 cm^{-1}. Initially (60 ns) the spectrum is dominated by two narrow band of phonon peaks at 43 and 70 cm^{-1} on a low broadband background. After 360 ns these features have increased in height and a third peak at 23 cm^{-1} has evolved. On a microsecond time scale the peak at 70 cm^{-1} decays while the lower energy features show little further time evolution. Time-resolved phonon spectra obtained after generation at 43 cm^{-1} (Fig. 3) show the build up of narrow-band phonon populations at both 20 and 23 cm^{-1}. We note that although the initial phonon population is resonant with an electronic state, the rise time of the phonon populations at both 20 and 23 cm^{-1} is 1.2 μs as opposed to <1 ns as expected for direct process relaxation between electronic states of this energy separation. Phonon generation at 66.0 and 111 cm^{-1} also resulted in phonon distributions which were highly peaked at 23 and 43 cm^{-1}.

Evolution of these narrow-band phonon distributions can be understood in terms of inelastic scattering of the original narrow-band phonon off the 23 and 43 cm^{-1} states as shown in Fig. 1(c). Here a phonon of frequency ν_{ph} causes an electronic transition of frequency δ yielding a phonon with the difference frequency ν_{ph}-δ. The electronic excitation then relaxes by rapid one-phonon emission to yield a phonon of frequency δ. We therefore attribute the peak observed at 70 cm^{-1} in Fig. 2 to the difference frequency phonons generated by inelastic scattering of 113-cm^{-1} phonons off the 43-cm^{-1} state,

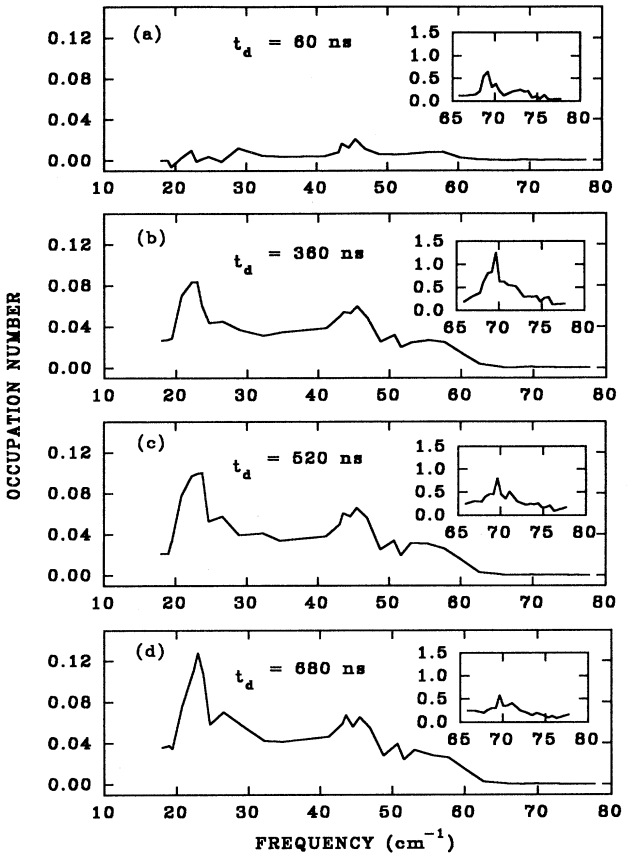

FIG. 2. Time-resolved phonon spectra after monochromatic phonon generation at 113 cm^{-1}. The insets show the evolution of the difference frequency phonons at 70 cm^{-1}. The occupation numbers of the insets have been multiplied by 10^3.

and the 20 cm^{-1} phonons observed in Fig. 3, to the difference frequency phonons generated by inelastic scattering of 43-cm^{-1} phonons off the 23-cm^{-1} state, respectively. We note that no inelastic scattering was observed off states attributed to Pr^{3+} ion in regular sites (19 and 50 cm^{-1}) even though these sites are present in greater numbers than the distorted sites. We believe that it is not unreasonable that ions in distorted sites exhibit a greater phonon scattering cross section, this is consistent with the pair state model for ruby which predicts that the inelastic scattering is dominated by Cr^{3+} pairs.[7]

We note that these peaks are not an artifact of the enhanced detection sensitivity which occurs at an electronic state due to an increased absorption cross section, as this is taken into account by our anti-Stokes normalization technique. Neither can these peaks be explained in terms of phonon bottlenecking, as an estimation of the distorted site concentration from a comparison of the line strengths of the 23 and 43 cm^{-1} lines with the resonant ground state to $^3P_0$ transitions predict a phonon bottlenecking factor of <1 for these states. With low bottlenecking factors a simple rate equation analysis shows that the electronic occupation number closely follows the resonant phonon occupation number. Further evidence that bottlenecking is not important here is provided in that

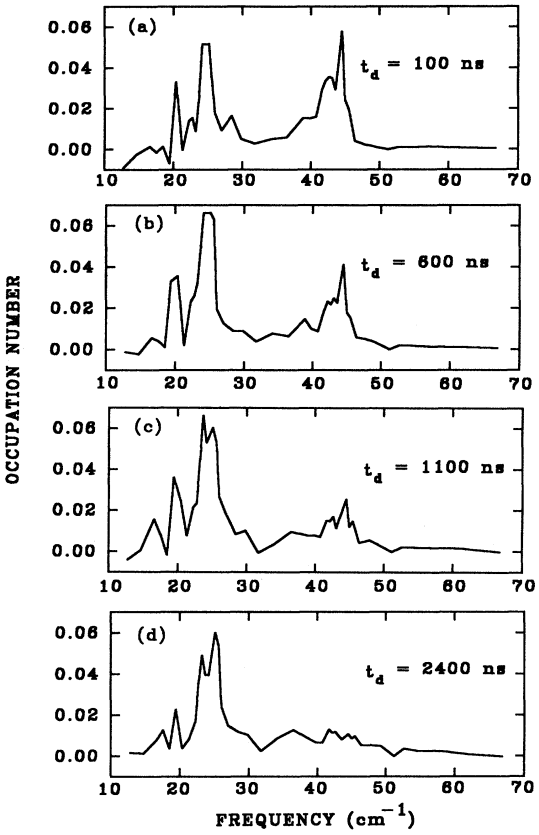

FIG. 3. Time-resolved phonon spectra after monochromatic phonon generation at 43 cm^{-1}.

there is no dramatic change of lifetime observed between the resonant phonons and phonons with nearby energies, for example the lifetimes of 39 and 43 cm^{-1} phonons are 1.6 and 1.3 μs, respectively.

In the presence of inelastic scattering the phonon lifetime should deviate from the ν^{-5} dependence expected for anharmonic decay.[8] The low-frequency data was found to tend asymptotically to a ν^2 dependence as shown in Fig. 4. The exact form of the approximations that lead to this behavior are currently under investigation. The solid line through the data shows the best fit of Eq. (3) to the experimental data.

$$t_d = \frac{1}{a\nu^5 + b\nu^2}, \tag{3}$$

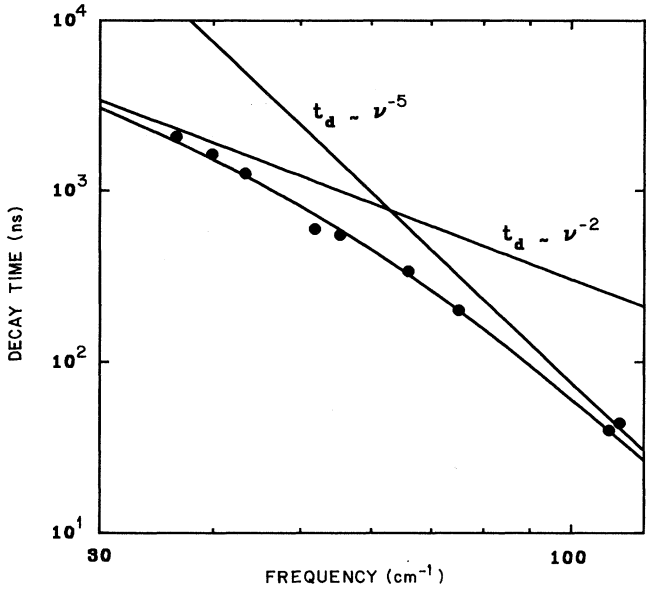

FIG. 4. Plot of phonon decay time vs phonon wave number. The smooth curve is the best fit of Eq. (3) to the data. The straight lines show the respective contributions of anharmonic and inelastic-scattering processes to the phonon decay.

where a and b were determined to be 1.32×10^{-3} $(cm^{-1})^{-5}s^{-1}$ and 3.29×10^{2} $(cm^{-1})^{-2}s^{-1}$, respectively.

We note that the anharmonic decay times in YAG are substantially longer than those observed previously in LaF_3.[3] This reduction in decay rate can be accounted for by the higher Debye frequency in YAG. No evidence was found that would indicate a significant interaction between the nonequilibrium phonons and the thermal phonon distribution at 16 K.

In conclusion, we have used DIOPA to investigate the decay of narrow-band nonequilibrium phonon distributions in YAG:Pr^{3+}. Phonon decay in this system appears to be dominated by inelastic phonon scattering off electronic transitions at distorted impurity sites. This mechanism leads to the evolution of phonon spectra which are highly peaked at the scattering frequencies.

This work was supported by National Science Foundation Grant No. DMR 8717696 and No. DMR 8914955.

[1] *Nonequilibrium Phonons in Nonmetallic Crystals,* edited by W. Eisenmenger and A. A. Kaplyanskii (North-Holland, Amsterdam, 1986), Chap. 3.

[2] H. J. Maris, Phys. Rev. B **41**, 9736 (1990).

[3] W. A. Tolbert, W.M. Dennis, and W. M. Yen, Phys. Rev. Lett. **65**, 607 (1990).

[4] R. S. Meltzer, J. E. Rives, and G. S. Dixon, Phys. Rev. B **28**, 4786 (1983).

[5] L. D. Rotter, W. M. Dennis, and W. M. Yen, Phys. Rev. B **42**, 720 (1990).

[6] W. A. Tolbert, W. M. Dennis, and W. M. Yen, Phys. Rev. B (to be published).

[7] S. Majetich, R. S. Meltzer, and J. E. Rives, Phys. Rev. B **38**, 11075 (1988).

[8] R. Orbach and L. A. Vredevoe, Physics (Long Island City, N.Y.) **1**, 91 (1964).